ELSEVIER

Chemical Engineering Journal 139 (2008) 462–468

Chemical Engineering Journal

www.elsevier.com/locate/cej

Chemical modification of multiwalled carbon nanotubes for sorption of Zn^{2+} from aqueous solution

Chungsying Lu *, Huantsung Chiu

Department of Environmental Engineering, National Chung Hsing University, 250 Kuo Kuang Road, Taichung 402, Taiwan

Received 12 November 2005; received in revised form 10 December 2006; accepted 9 August 2007

Abstract

Multiwalled carbon nanotubes (MWCNTs) were oxidized by mixed HNO_3/H_2SO_4 (3N + 1S), HNO_3, $KMnO_4$ and NaClO and were selected as sorbents to study their characterization and isotherm of Zn^{2+} sorption in an aqueous solution. The physicochemical properties of MWCNTs were improved after oxidation, which made MWCNTs possess not only a more hydrophilic surface but also a more negatively charged surface, and consequently resulted in sorption of more Zn^{2+}. The maximum Zn^{2+} sorption capacities of MWCNTs, MWCNTs(3N + 1S), MWCNTs(HNO_3), MWCNTs($KMnO_4$) and MWCNTs(NaClO) calculated by Langmuir model are 10.21, 18.14, 27.20, 28.01 and 32.68 mg g^{-1}, respectively. The MWCNTs(NaClO) have the best sorption performance of Zn^{2+} and their sorption kinetics was found to follow the pseudo second-order rate law.

Keywords: Multiwalled carbon nanotubes; Chemical oxidation; Surface functional groups; Zn^{2+} sorption

1. Introduction

Carbon nanotubes (CNTs) are unique and one-dimensional macromolecules that have outstanding thermal and chemical stability [1]. These nanomaterials have been proven to possess great potential as superior adsorbents for removing many kinds of organic and inorganic pollutants in air streams or from aqueous environments [2–9]. The large adsorption capacity of CNTs is mainly attributable to their pore structure, surface area and the existence of a wide spectrum of surface functional groups. A modification of CNTs with specific physicochemical properties can be achieved by chemical or thermal treatments to make CNTs that have optimal performance for particular purposes. Therefore, a test on the modification method of CNTs is needed for employing the most efficient CNTs in order to meet the growing demand for cleaner air and water.

Chemical oxidations have produced activated carbons with weakly acidic functional groups [10], which can provide numerous chemical sorption sites and consequently enhance the affinity for metal ions as compared to the parent carbons. Chemical oxidations that apply to activated carbons would be expected to CNTs.

In this paper, multiwalled carbon nanotubes (MWCNTs) were oxidized by various kinds of chemical agents and were employed as sorbents to study their characterization. Isotherms and kinetics of Zn^{2+} sorption in an aqueous solution, which is commonly discharged from many kinds of industrial activities such as chemicals, metals, pulp and paper manufacturing processes [11], were also conducted to determine the optimal chemical modification of MWCNTs in water and wastewater treatment.

2. Materials and methods

2.1. Sorbents

MWCNTs with outer diameter (dp) ≤10 nm (L-type, Nanotech Port Co., Shenzhen, China) were selected as sorbents in this study. The length of MWCNTs was in the range 5–15 μm and the amorphous carbon content in the MWCNTs was <5%. These data were provided by the manufacturer.

Raw MWCNTs were thermally treated using an oven at 350 °C for 30 min to remove amorphous carbons. After this thermal treatment, MWCNTs were oxidized by various kinds of chemical agents including HCl, H_2SO_4, H_2O_2, O_3, 30 mL HNO_3 + 10 mL H_2SO_4 (3N + 1S), HNO_3, $KMnO_4$ and NaClO. Literature screening shows that these chemical agents have been

* Corresponding author. Fax: +886 4 2286 2587.
E-mail address: clu@nchu.edu.tw (C. Lu).

1385-8947/$ – see front matter © 2007 Elsevier B.V. All rights reserved.
doi:10.1016/j.cej.2007.08.013

used to modify carbon adsorbents for the removal of metal ions from aqueous solution [4,8,10,12]. The oxidation procedure has been provided elsewhere [8].

2.2. Sorbate

Analytical-grade zinc nitrate (Merck Ltd., Taipei, Taiwan, 96–97% purity) was employed to prepare a stock solution containing 1 g L^{-1} of Zn^{2+}. The stock solution was further diluted with deionized water to the desired Zn^{2+} concentrations. The use of deionized water was to prevent the effect of solution ionic strength.

2.3. Batch sorption experiments

Batch sorption experiments were conducted using 150 mL glass bottles with addition of 0.05 g of MWCNTs and 100 mL of Zn^{2+} solution of initial concentrations (C_0) from 10 to 80 mg L^{-1}. The concentration ranges were chosen to be representative of Zn^{2+} concentrations in raw water and wastewater. The glass bottles were sealed with 20 mm rubber stopper and then were mounted on a shaker, which was placed in a temperature-controlled box (model CH-502, Chin Hsin, Taipei, Taiwan) and operated at 25 °C and 180 rpm for 12 h. The choice of agitation speed of 180 rpm was to provide a high degree of mixing while the selection of contact time of 12 h was to assure the attainment of sorption equilibrium. All the experiments were triplicated, and only the mean values were reported. The maximum deviation is less than 5%. Blank test was conducted without addition of sorbents, and the results showed that only very little Zn^{2+} uptakes by the glass bottle wall were occurring, which had no influence on the sorption experiments. The initial solution pH was adjusted at neutrality by using 0.1 M HNO_3 or 0.1 M NaOH, in which the predominant zinc species is always Zn^{2+} [13].

The amount of sorbed Zn^{2+} was calculated as follows:

$$q = (C_0 - C_t) \times \frac{V}{m} \quad (1)$$

where q is the amount of Zn^{2+} sorbed onto MWCNTs (mg g^{-1}); C_0 is the initial Zn^{2+} concentration (mg L^{-1}); C_t is the Zn^{2+} concentration after a certain period of time (mg L^{-1}); V is the initial solution volume (L); and m is the CNT mass (g).

2.4. Analytical methods

The concentration of Zn^{2+} was determined by a flame atomic absorption spectrometer (FAAS, Model 100, Perkin-Elmer, USA). The morphology of MWCNTs was analyzed by a field emission scanning electron microscope (FE-SEM, JEOL JSM-6700, Tokyo, Japan) and a high-resolution transmission electron microscope (HR-TEM, JEOL JEM-2010, Tokyo, Japan).

The physical properties of sorbents were determined by nitrogen adsorption at 77 K using ASAP 2010 surface area analyzers (Micromertics Inc., Norcross, GA, USA). N_2 adsorption isotherms were measured at a relative pressure range 0.0001–0.99. The adsorption data were then employed to determine surface area using the Brunauer, Emmett, and Teller equation and pore size distribution (including average pore diameter and pore volume) using the Barrett, Johner, and Halenda equation.

The functional groups on the surface site of sorbents were detected by a Fourier transform infrared spectroscometer (model FT/IR-200, JAS Co., Tokyo, Japan). The carbon content of the sorbents was determined by a thermogravimetric analyzer (model Labsys TG-DSC 131, Setaram Instrumentation, Galuire, France). The structural information of sorbents was evaluated by a Raman spectrometer (model Nanofinder 30 R., Tokyo Instruments Inc., Tokyo, Japan).

Zeta potentials of sorbents were measured across the solution pH range 2–12. Samples were prepared identically to those of the batch experiments. Thirty measurements were made for each sample on a Malvern Zetasizer (model ZEN 1001, Malvern Co., UK) and the average was taken as the zeta potential of the sorbents. The isoelectric point (pH_{iep}) of sorbents, the pH at which the positive surface charge equals the negative surface charge, can be determined from these measurements.

3. Results and discussion

3.1. Zn^{2+} sorption performance of various oxidized MWCNTs

Fig. 1 shows the amount of Zn^{2+} sorbed onto various oxidized MWCNTs at equilibrium (q_e) with a C_0 of 30 mg L^{-1}. The q_e of HCl, H_2SO_4, H_2O_2, O_3, 3N + 1S, HNO_3, $KMnO_4$ and NaClO oxidized MWCNTs are 2.72, 3.52, 5.01, 7.03, 13.6, 18.48, 21.61 and 25.52 mg g^{-1}, respectively. It is apparent that the 3N + 1S, HNO_3, $KMnO_4$ and NaClO oxidized MWCNTs have better sorption performance of Zn^{2+} than the other oxidized MWCNTs, and consequently they were selected as sorbents to study their characterization and isotherm of Zn^{2+} sorption in an aqueous solution.

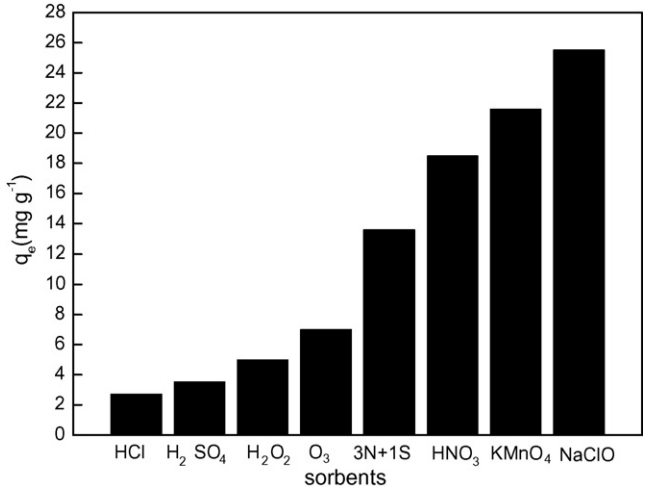

Fig. 1. Amount of Zn^{2+} sorbed onto oxidized MWCNTs at equilibrium.

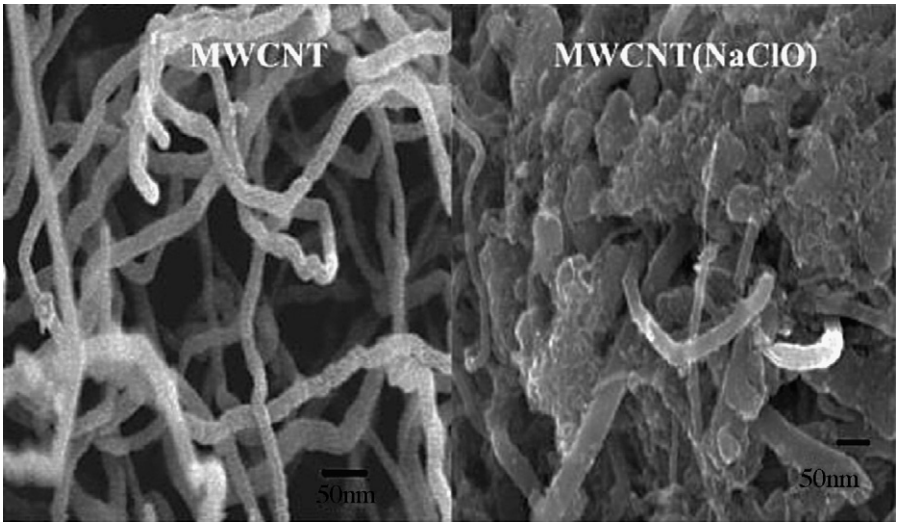

Fig. 2. SEM images of raw and NaClO oxidized MWCNTs.

3.2. Characterization of oxidized MWCNTs

3.2.1. Microscope images

Fig. 2 displays the SEM images of raw and NaClO oxidized MWCNTs. It is seen that the isolated MWCNTs usually curve and have cylindrical shapes with an external diameter of ~25 nm. Due to inter-molecular force, the isolated MWCNTs of different size and direction form an aggregated structure. Thus, the lengths of the MWCNTs are difficult to determine definitively, but are in the range of hundreds of nanometers to micrometers. The confined space among isolated MWCNTs becomes narrow after oxidation.

Fig. 3 exhibits the TEM images of raw and NaClO oxidized MWCNTs. The MWCNT contained a concentrically nested array of single-walled carbon nanotubes with an outer diameter of <10 nm and with the hollow inner tube diameter of ~4 nm. A large amount of metal catalysts and amorphous carbons appeared within MWCNTs and was removed after oxidation, which results in the decrease in the extent of carbon-containing defects along the surface of oxidized MWCNTs.

The SEM and TEM images of other oxidized MWCNTs show similar results to that of NaClO oxidized MWCNTs.

3.2.2. FTIR spectra

Fig. 4 presents the IR spectra of raw and oxidized MWCNTs. The IR spectra of oxidized MWCNTs show four major peaks at ~3750, 3450, 2370 and 1562 cm^{-1}. The peak at ~3750 is attributed to free hydroxyl groups [14]. The peak at ~3450 cm^{-1} can be assigned to –OH stretch from carboxylic groups (–COOH and –COH) while the peak at ~2370 cm^{-1} can be associated with –OH stretch from strongly H-bond-COOH [15]. The peak at ~1562 cm^{-1} is related to the carboxylate anion stretch mode [16]. These oxygen-containing functional groups produced are abundant on the external and internal surface of MWCNTs, which can provide numerous chemical sorption sites and thus increase the ion-exchange capacity for Zn^{2+}. The

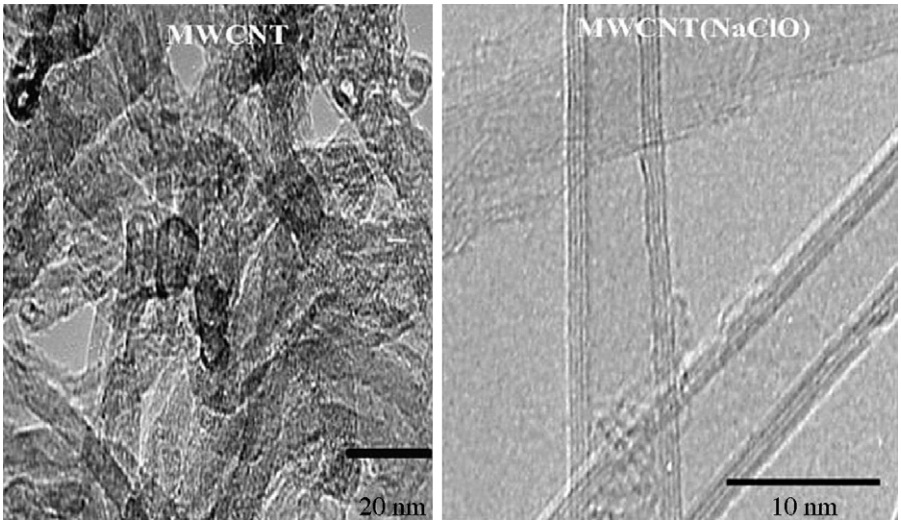

Fig. 3. TEM images of raw and NaClO oxidized MWCNTs.

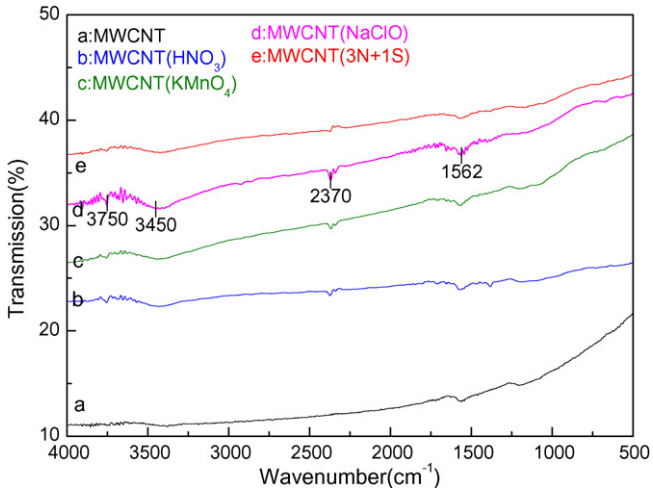

Fig. 4. Fourier transform infrared spectra of raw and oxidized MWCNTs.

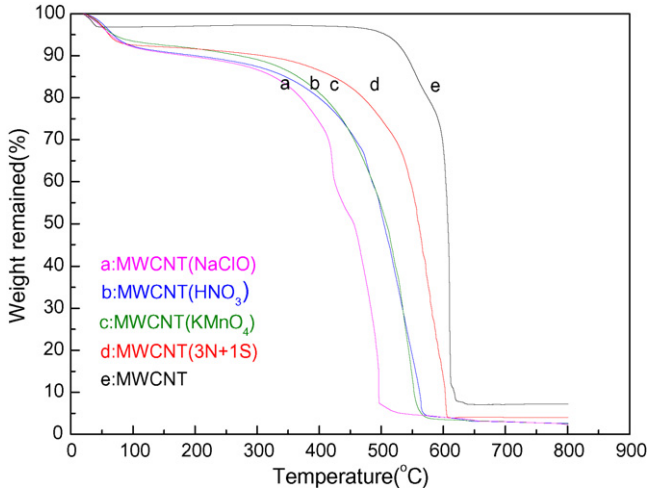

Fig. 6. Thermogravimetric analyses of raw and oxidized MWCNTs.

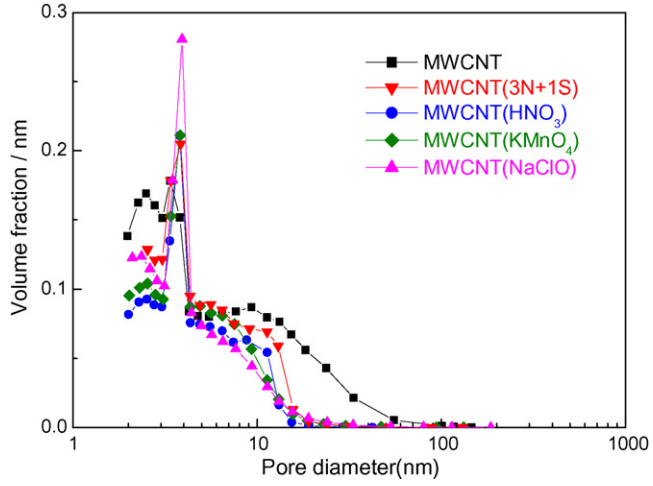

Fig. 5. Pore size distributions of raw and oxidized MWCNTs.

IR spectrum of raw MWCNTs only exhibits a major peak at 1562 cm^{-1}.

3.2.3. BET measurement

Fig. 5 shows the pore size distributions of raw and oxidized MWCNTs. Pore size distributions of raw and oxidized MWCNTs can be characterized into a fine fraction ($2 \leq$ pore size ≤ 4 nm) and a coarse fraction (pore size > 4 nm). The pores in the fine fraction are the MWCNT inner cavities, close to the inner MWCNT diameter while the pores in the coarse fraction are likely to be contributed by aggregated pores which are formed within the confined space among the isolated MWCNTs. Pore size distributions of four oxidized MWCNTs are very similar.

It is clear that the raw MWCNTs possess larger volume fraction of inner cavities and aggregated pores than the oxidized MWCNTs. The decrease in the volume fraction of inner cavities after oxidation could be attributed to the pore entrance blockage by the formation of functional groups. The decrease in the volume fraction of aggregated pores could be explained by the fact that the confined space of isolated MWCNTs becomes narrow after oxidation as shown in SEM images.

The physical properties of raw and oxidized MWCNTs are given in Table 1. As can be observed, the raw MWCNTs have greater surface area, average pore diameter and pore volume than the oxidized MWCNTs. Most pore volumes of raw MWCNTs are in the size > 10 nm while most pore volumes of oxidized MWCNTs are in the 2–10 nm width range.

3.2.4. TGA

Fig. 6 reveals the TGA results of raw and oxidized MWCNTs. It is evident that the raw MWCNTs are considerably stable and show a little weight loss close to 5% below 500 °C. A significant gasification of MWCNTs begins at 500 °C and ends at 610 °C, in which 7.21% remaining weight was found. The oxidized MWCNTs have a broader temperature range for weight loss than the

Table 1
Physical properties of sorbents

Sorbents	Surface area ($m^2\ g^{-1}$)	Ave. pore diameter (nm)	Pore volume ($cm^3\ g^{-1}$)	% of total pore volume in stated pore size (nm) range		
				2–5	5–10	>10
MWCNT	435	8.35	0.91	17.4	18.2	64.4
MWCNT(3N + 1S)	330	5.88	0.48	36.6	35.5	27.9
MWCNT(HNO_3)	256	5.60	0.35	41.6	40.1	18.3
MWCNT($KMnO_4$)	283	5.52	0.37	40.3	38.8	20.9
MWCNT(NaClO)	297	5.17	0.38	45.1	29.6	25.3

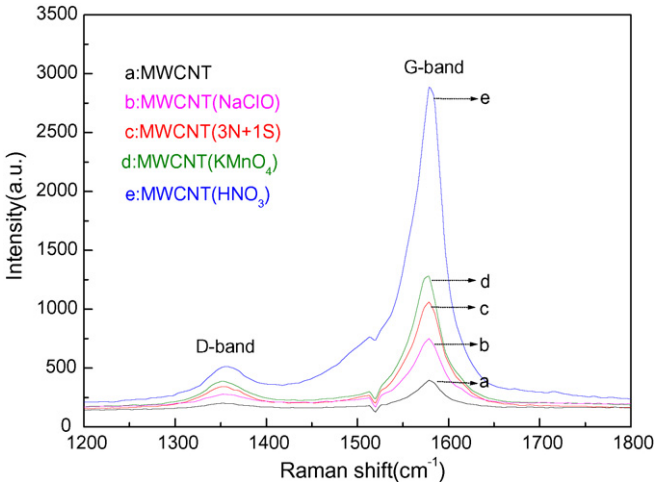

Fig. 7. Raman spectra of raw and oxidized MWCNTs.

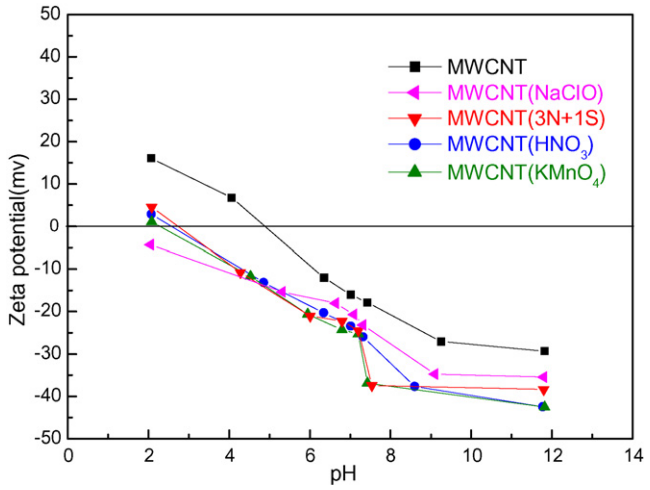

Fig. 8. Zeta potentials of raw and oxidized MWCNTs under various solution pH.

MWCNTs and exhibit three main weight loss regions. The first weight loss region can be attributed to the loss of various kinds of functional groups on the surface of MWCNTs. The rapid weight loss region can be assigned to the decomposition of MWCNTs. The third region only shows a very little weight loss close to 2%, in which 4.04, 2.58, 2.48 and 2.35% remaining weight was observed for the MWCNTs(3N + 1S), MWCNTs(HNO_3), MWCNTs($KMnO_4$) and MWCNTs(NaClO). This reflects that the carbon content in the MWCNTs increases from 92.79 to 95.96, 97.42, 97.52 and 97.65% after oxidation by 3N + 1S, HNO_3, $KMnO_4$ and NaClO solution, respectively, which could be attributed to the removal of amorphous carbons and metal catalysts after oxidation as shown in TEM images. Similar TGA results have been reported for the crude MWCNTs and functionalized MWCNTs [17].

3.2.5. Raman spectra

The Raman spectra of raw and oxidized MWCNTs presented in Fig. 7 are composed of two characteristic peaks. The peak near 1350 cm^{-1} is the D band corresponding to the disordered sp^2-hybridized carbon atoms of nanotubes while the peak near 1580 cm^{-1} is the G band corresponding to the structural integrity of sp^2-hybridized carbon atoms of nanotubes. Together, these bands can be used to evaluate the extent of carbon-containing defects [18–20]. The intensity ratios of D band to G band (I_D/I_G) of raw and oxidized MWCNTs are given in Table 2. As can be observed, the raw MWCNTs have a higher I_D/I_G ratio than the oxidized MWCNTs. This suggests that the raw MWCNTs contain more amorphous carbon and multishell sp^2-hybridized carbon nanoparticles that can encapsulate residual metal catalysts. In other words, the raw MWCNTs have less crystalline graphitic structures, which are consistent with the TEM images and the TGA results.

Table 2
I_D/I_G ratios of sorbents

Sorbents	I_D/I_G
MWCNT	0.5037
MWCNT(3N + 1S)	0.3232
MWCNT(HNO_3)	0.1764
MWCNT($KMnO_4$)	0.3040
MWCNT(NaClO)	0.3706

3.2.6. Zeta potentials

Fig. 8 shows the zeta potentials of raw and oxidized MWCNTs under various solution pH. As the solution pH increased, the surface charge of MWCNTs became more negative, likely because of the deposition of more hydroxide ions on the surface of MWCNTs. The MWCNTs(NaClO) exhibit all negative surface charges within the pH range tested herein. The MWCNTs($KMnO_4$), MWCNTs(HNO_3), MWCNTs(3N + 1S) and MWCNTs show the pH_{iep} of 2.25, 2.6, 2.75 and 4.9, respectively, indicating that the surface of these MWCNTs maintained acidic characteristics. The oxidized MWCNTs possess more negative surface charges than the raw MWCNTs, probably because of the presence of more negatively charged surface functional groups as shown in FTIR spectra. From an electrostatic interaction point of view, sorption of Zn^{2+} onto MWCNTs, MWCNTs(3N + 1S), MWCNTs(HNO_3), MWCNTs($KMnO_4$) and MWCNTs(NaClO) is favored for solution pH > 4.9, 2.75, 2.6, 2.25 and 2.0 respectively.

3.3. Isotherm models

The q_e are correlated with isotherm models of Langmuir [21] and Freundlich [22],

$$q_e = \frac{abC_e}{1 + bC_e} \quad (2)$$

$$q_e = K_f C_e^{1/n} \quad (3)$$

where C_e is the equilibrium concentration of Zn^{2+} (mg L^{-1}); a is the maximum sorption capacity (mg g^{-1}); b is the Langmuir sorption constant (L mg^{-1}); and K_f and n are the Freundlich constants. The constants of Langmuir and Freundlich models were obtained from fitting the model to the q_e and are given in Table 3.

Table 3
Constants of Langmuir and Freundlich models

Sorbents	Langmuir model			Freundlich model		
	a	b	R^2	K_f	$1/n$	R^2
MWCNT	10.21	0.0077	0.471	0.17	0.714	0.928
MWCNT(3N + 1S)	18.14	0.13	0.997	6.25	0.237	0.991
MWCNT(HNO_3)	27.20	0.15	0.999	6.14	0.339	0.950
MWCNT($KMnO_4$)	28.01	0.16	0.997	9.89	0.236	0.982
MWCNT(NaClO)	32.68	0.22	0.999	11.84	0.244	0.940

Units: a = mg g^{-1}; b = L mg^{-1}; K_f = (mg g^{-1})(L mg^{-1})$^{1/n}$; n, R = dimensionless.

With the exception of raw MWCNTs, the q_e of oxidized MWCNTs are better correlated with Langmuir model. The a and K_f, which represent the Zn^{2+} sorption capacity, are the greatest for the MWCNTs(NaClO), followed by the MWCNTs($KMnO_4$), MWCNTs(HNO_3), MWCNTs(3N + 1S) and then the MWCNTs. The constant b, which is related to the free energy of sorption, presents the same trend as the a and K_f, indicating that the oxidized MWCNTs have a higher affinity for Zn^{2+} than the raw MWCNTs.

Langmuir isotherms of Zn^{2+} onto raw and oxidized MWCNTs are presented in Fig. 9. The Zn^{2+} sorption onto MWCNTs was greatly improved after oxidation by 3N + 1S, HNO_3, $KMnO_4$ and NaClO solutions, reflecting that oxidation of MWCNTs is required for better performance for sorption of Zn^{2+} from aqueous solution. This could be because of the changes in the physicochemical properties of MWCNTs including the increase in carbon content in the MWCNTs, surface functional groups and negatively charged carbon surfaces. These modifications made MWCNTs provide not only a more hydrophilic surface but also a more negatively charged surface.

The a values of MWCNTs, MWCNTs(3N + 1S), MWCNTs(HNO_3), MWCNTs($KMnO_4$) and MWCNTs (NaClO) are 10.21, 18.14, 27.20, 28.01 and 32.68 mg g^{-1}, respectively. The MWCNTs(NaClO) are the most effective Zn^{2+} sorbents, followed by the MWCNTs($KMnO_4$), MWCNTs(HNO_3), MWCNTs(3N + 1S), and then the MWCNTs. Although the MWCNTs have 1.3–1.7 times more surface areas and 1.9–2.6 times greater pore volumes than the oxidized MWCNTs, the oxidized MWCNTs possess 1.8–3.2 times more a than the MWCNTs. This reflects that Zn^{2+} sorption onto MWCNTs is dependent on chemical interactions between the Zn^{2+} and the surface functional groups of MWCNTs rather than surface area and pore volume of MWCNTs. Similar findings have been reported in the literature for sorption of Zn^{2+} onto activated carbons [13]. The MWCNTs(NaClO) were consequently selected as sorbents to study the kinetics of Zn^{2+} sorption in an aqueous solution.

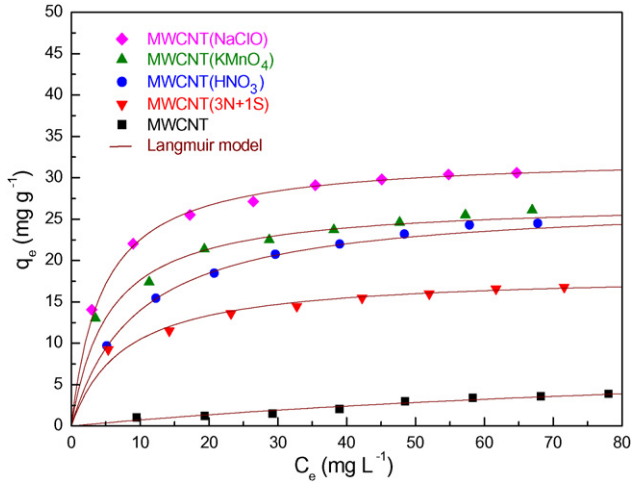

Fig. 9. Langmuir isotherm of Zn^{2+} sorption onto raw and oxidized MWCNTs.

3.4. Kinetic study

Effects of contact time on the Zn^{2+} sorption of MWCNTs(NaClO) with a C_0 of 10 and 60 mg L^{-1} were investigated. The Zn^{2+} sorption increased quickly with time and then slowly reached equilibrium in 20 and 60 min with a C_0 of 10 and 60 mg L^{-1}, respectively, in which the q_e are 14.16 and 28.8 mg g^{-1}. It is apparent that the equilibrium would be reached faster at a lower C_0, probably because the sorption sites of MWCNTs(NaClO) sorbed the available Zn^{2+} more rapidly at a lower C_0.

To analyze the sorption rate of Zn^{2+} onto MWCNTs(NaClO), the pseudo second-order rate equation is employed [23,24]:

$$\frac{t}{q_t} = \frac{1}{(k_2 q_e^2)} + \frac{t}{q_e} \quad (4)$$

where q_t is the amount of Zn^{2+} sorbed onto MWCNTs at time t (mg g^{-1}); and k_2 is the pseudo second-order rate constant (g mg^{-1} min^{-1}). The q_e and k_2 were calculated from the slope and the intercept of a linear plot of t/q_t versus t and, respectively, are 14.4 mg g^{-1} and 0.0121 g mg^{-1} min^{-1} with a C_0 of 10 mg L^{-1} and 28.16 mg g^{-1} and 0.0083 g mg^{-1} min^{-1} with a C_0 of 60 mg L^{-1}. The correlation coefficients are all >0.999, indicating that the kinetics of Zn^{2+} sorption onto MWCNTs follows the pseudo second-order rate law. The calculated and experimental q_e are very close with the deviation ~2%.

4. Conclusions

The 3N + 1S, HNO_3, $KMnO_4$ and NaClO oxidized MWCNTs were selected as sorbents to study their characterization and isotherm of Zn^{2+} sorption in an aqueous solution. The physicochemical properties of MWCNTs were improved after oxidation including the increase in carbon content in the MWCNTs, oxygen-containing functional groups and negatively charged carbon surfaces. These modifications made MWCNTs possess a better sorption performance of Zn^{2+}. The MWCNTs(NaClO) appear to be the most effective Zn^{2+} sorbents, followed by the MWCNTs($KMnO_4$), MWCNTs(HNO_3), MWCNTs(3N + 1S), and then the MWCNTs. The kinetics of Zn^{2+} sorption onto MWCNTs(NaClO) was found to follow the pseudo second-order rate law.

Acknowledgement

Support from the National Science Council, Taiwan, under a contract no. NSC 94-2211-E-005-038 is gratefully acknowledged.

References

[1] S.K. Smart, A.I. Cassady, G.Q. Lu, D.J. Martin, The biocompatibility of carbon nanotubes, Carbon 44 (2006) 1034–1047.
[2] Q.R. Long, R.T. Yang, Carbon nanotubes as superior sorbent for dioxin removal, J. Am. Chem. Soc. 123 (2001) 2058–2059.
[3] Y.H. Li, S. Wang, J. Wei, X. Zhang, C. Xu, Z. Luan, D. Wu, B. Wei, Lead adsorption on carbon nanotubes, Chem. Phys. Lett. 357 (2002) 263–266.
[4] Y.H. Li, S. Wang, Z. Luan, J. Ding, C. Xu, D. Wu, Adsorption of cadmium(II) from aqueous solution by surface oxidized carbon nanotubes, Carbon 41 (2003) 1057–1062.
[5] Y.H. Li, S. Wang, J. Wei, X. Zhang, C. Xu, Z. Luan, D. Wu, Adsorption of fluoride from water by aligned carbon nanotubes, Mater. Res. Bull. 38 (2003) 469–476.
[6] X. Peng, Y. Li, Z. Luan, Z. Di, H. Wang, B. Tian, Z. Jia, Adsorption of 1,2 dichlorobenzene from water to carbon nanotubes, Chem. Phys. Lett. 376 (2003) 154–158.
[7] C. Lu, Y.L. Chung, K.F. Chang, Adsorption of trihalomethanes from water with carbon nanotubes, Water Res. 39 (2005) 1183–1189.
[8] C. Lu, H. Chiu, Adsorption of zinc(II) from water with purified carbon nanotubes, Chem. Eng. Sci. 61 (2006) 1134–1141.
[9] C. Lu, C. Liu, Removal of nickel(II) from aqueous solution by carbon nanotubes, J. Chem. Technol. Biotechnol. 81 (2006) 1932–1940.
[10] P. Chingombe, B. Saha, R.J. Wakeman, Surface modification and characterization of a coal-based activated carbon, Carbon 43 (2005) 3132–3143.
[11] W.W. Eckenfelder, Industrial Water Pollution Control, McGraw-Hill International Edition, Singapore, 1989.
[12] S. Biniak, M. Pakula, G.S. Szymanski, A. Swiatkowski, Effect of activated carbon surface oxygen and/or nitrogen-containing groups on adsorption of copper(II) ions from aqueous solution, Langmuir 15 (1999) 6117–6122.
[13] R.R. Leyva, J.L.A. Bernal, B.J. Mendoza, R.L. Fuentes, C.R.M. Guerrero, Adsorption of zinc(II) from an aqueous solution onto activated carbon, J. Hazard. Mater. B90 (2002) 27–38.
[14] H.Y. Huang, R.T. Yang, D. Chinn, C.L. Munson, Amine-grafted MCM-48 and silica xerogel as superior sorbents for acid gas removal from natural gas, Ind. Eng. Chem. Res. 42 (2003) 2427–2433.
[15] W.M. David, C.L. Erickson, C.T. Johnston, J.J. Delfino, J.E. Porter, Quantitative fourier transform infrared spectroscopic investigation of humic substance functional group composition, Chemosphere 38 (1999) 2913–2928.
[16] G. Ovejero, J.L. Sotelo, M.D. Romero, A. Rodríguez, M.A. Ocaña, G. Rodríguez, J. García, Multiwalled carbon nanotubes for liquid-phase oxidation. Functionalization, characterization, and catalytic activity, Ind. Eng. Chem. Res. 45 (2006) 2206–2212.
[17] J. Cui, W.P. Wang, Y.Z. You, C. Liu, P. Wang, Functionalization of multiwalled carbon nanotubes by reversible addition fragmentation chain-transfer polymerization, Polymer 45 (2004) 8717–8721.
[18] C.L. Tsai, C.F. Chen, Characterization of bias-controlled carbon nanotubes, Diamond Relat. Mater. 12 (2003) 1615–1620.
[19] M.S. Dresselhaus, G. Dresselhaus, A. Jorio, A.G. Souza Filho, R. Saito, Raman spectroscopy on isolated single wall carbon nanotubes, Carbon 40 (2002) 2043–2061.
[20] C.J. Ko, C.Y. Lee, F.H. Ko, H.L. Chen, T.C. Chu, Highly efficient microwave-assisted purification of mulltiwalled carbon nanotubes, Microelectron. Eng. 73–74 (2004) 570–577.
[21] I. Langmuir, The constitution and fundamental properties of solids and liquids, J. Am. Chem. Soc. 38 (1916) 2221–2295.
[22] H.M.F. Freundlich, Über die adsorption in Iösungen, J. Phys. Chem. 57 (1906) 385–470.
[23] G. Blanchard, M. Maunaye, G. Martin, Removal of heavy metals from waters by means of natural zeolites, Water Res. 18 (1984) 1501–1507.
[24] Y.S. Ho, G. McKay, The kinetics of sorption of divalent metal ions onto sphagnum moss peat, Water Res. 34 (2000) 735–742.